Transient anomalous diffusion in run-and-tumble dynamics

M. Reza Shaebani* and Heiko Rieger

Department of Theoretical Physics & Center for Biophysics,
Saarland University, 66041 Saarbrücken, Germany

We study the stochastic dynamics of a particle with two distinct motility states. Each one is characterized by two parameters: one represents the average speed and the other represents the persistence quantifying the tendency to maintain the current direction of motion. We consider a run-and-tumble process, which is a combination of an active fast motility mode (persistent motion) and a passive slow mode (diffusion). Assuming stochastic transitions between the two motility states, we derive an analytical expression for the time evolution of the mean square displacement. The interplay of the key parameters and the initial conditions as for instance the probability of initially starting in the run or tumble state leads to a variety of transient regimes of anomalous transport on different time scales before approaching the asymptotic diffusive dynamics. We estimate the crossover time to the long-term diffusive regime and prove that the asymptotic diffusion constant is independent of initially starting in the run or tumble state.

I. INTRODUCTION

Many transport processes in nature involve distinct motility states. Of particular interest is the run-and-tumble process, which consists of alternating phases of fast active and slow passive motion. Prominent examples are bacterial species that swim when their flagella form a bundle and synchronize their rotation. The bundle is disrupted and swimming stops when some of the flagella stochastically change their rotational direction. In the absence of rotating bundle, the bacterium moves diffusively until it manages to re-form the bundle and actively move forward again [1, 2]. The run-and-tumble dynamics is beneficial for bacteria as it allows them to react to the environmental changes by adjusting their average run time or speed [3], change their direction of motion, perform an efficient search [4–7], or optimize their navigation [8, 9].

Another example is the motion of molecular motors along cytoskeletal filaments. When motor proteins bind to filaments, they perform a number of steps until they randomly unbind and experience diffusion in the crowded cytoplasm. While the efficiency of long-distance cargo delivery requires high motor processivity (i.e. the tendency to continue the motion along the filament), the slow diffusive mode during unbinding periods is also vital for cellular functions which depend on the localization of the reactants [10–13]. The processivity of the motors (and thus the unbinding probability) depends on the type of motor and filament [14, 15] and the presence of particular proteins or binding domains in the surrounding medium [16–18]. On the other hand other factors, such as cell crowding, may affect the binding probability. Therefore, the switching probabilities between active run and tumble states are generally asymmetric. By ignoring the microscopic details of stepping on filaments, coarse-grained random walk models have been employed

to study the two-state dynamics of molecular motors [19–22]. Dentritic immune cells also move persistently (migration phase) interrupted by slow phases for antigen uptake [23]. There have been many other locomotive patterns in biological and non-living systems investigated via models with distinct states of motility [24–31]. For instance, the problem of searcher proteins finding a specific target site over a DNA strand has been studied by multi-state stochastic processes [32–34].

The particle trajectories obtained from experiments often comprise a set of recorded positions of the particle, from which the successive directions of motion can be deduced. These directions are correlated on short time scales for active motions. However, the trajectory eventually gets randomized and the asymptotic dynamics is diffusive, with a diffusion constant D_{asymp} that depends on the particle velocity and persistency [35, 36]. One expects a similar long-term behavior for a mixture of run and tumble dynamics as well. The question arises how the transient short time dynamics, the crossover time to asymptotic diffusion, and D_{asymp} depend on the run and tumble velocities and the switching probabilities between the two states. It is also unclear how the overall dynamics is influenced by the choice of the initial conditions of motion, like the probabilities to start either in the run or tumble state, which are parameters that can be extracted from experimental data.

Here, we present a two-state model for the run-and-tumble dynamics with spontaneous switchings between the states of motility. By deriving an analytical expression for the time evolution of the mean square displacement, we show how the interplay between the run and tumble velocities, the transition probabilities, and the initial conditions of motion leads to various anomalous transport regimes on short and intermediate time scales. We particularly clarify how the probability of starting from run or tumble state diversifies the transient anomalous regimes of motion, and verify that the long-term diffusion constant D_{asymp} does not depend on the choice of the initial conditions of motion.
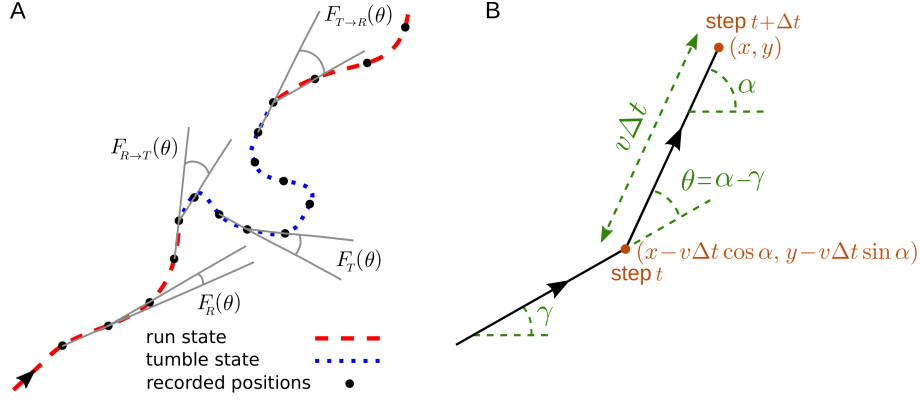
* shaebani@lusi.uni-sb.de

FIG. 1. (A) A sample trajectory with run-and-tumble dynamics. Typical turning angles for different types of turning-angle distributions introduced in the model are shown. (B) Trajectory of the walker during two successive steps.

II. MODEL

We develop a stochastic model for the run-and-tumble dynamics with spontaneous transitions between the motility states. We consider a two-state random walk in discrete time and continuous space with the following characteristics: The *run* phase is a persistent random walk with persistency p and mean speed v_{R}. The dynamics in the *tumble* phase is an ordinary diffusion with the mean speed v_{T}. The asymmetric transition probabilities from run to tumble phase and vice versa are denoted, respectively, by $f_{\mathrm{R}\to\mathrm{T}}$ and $f_{\mathrm{T}\to\mathrm{R}}$. As a result of constant transition probabilities, the run and tumble times are exponentially distributed in our model. This restriction can be relaxed by introducing time-dependent transition probabilities [37]. To characterize the persistency of the run phase, we use the probability distribution $F_{\mathrm{R}}(\theta)$ of directional changes along the trajectory in the run phase. The directional persistence can be characterized by the persistency parameter $p = \int_{-\pi}^{\pi} \mathrm{d}\theta \ e^{\mathrm{i}\theta} F_{\mathrm{R}}(\theta)$, which leads to $p = \langle \cos\theta \rangle$ for symmetric distributions with respect to the arrival direction. Thus, p ranges from 0 for pure diffusion to 1 for ballistic motion and reflects the average curvature of the run trajectories. Similarly, we define $F_{\mathrm{T}}(\theta)$ for the probability distribution of directional changes along the trajectory in the tumble phase, and $F_{\mathrm{R}\to\mathrm{T}}(\theta)$ and $F_{\mathrm{T}\to\mathrm{R}}(\theta)$ for the directional changes when switching between the states occurs [see Fig. 1(A)]. In the tumble phase (i.e. an ordinary diffusion), the probability distribution of directional changes is isotropically distributed ($F_{\mathrm{T}}(\theta) = \frac{1}{2\pi}$), leading to a zero persistency.

The run-and-tumble stochastic process can be described in discrete time by introducing the probability densities $P_t^R(x,y|\alpha)$ and $P_t^T(x,y|\alpha)$ to find the particle at position (x,y) arriving along the direction α at time t in the run and tumble states, respectively. α is defined with respect to a given reference direction, as shown in Fig. 1(B). Denoting the time interval between consecutive recorded positions of the particle by Δt, the following

set of master equations describe the dynamical evolution of the probability densities

$$P_{t+\Delta t}^R(x,y|\alpha) =$$

$$(1-f_{\mathrm{R}\to\mathrm{T}})\int_{-\pi}^{\pi} d\gamma\, F_{\mathrm{R}}(\alpha-\gamma) P_t^R(x-v_{\mathrm{R}}\Delta t\cos\alpha, y-v_{\mathrm{R}}\Delta t\sin\alpha|\gamma)$$

$$+f_{\mathrm{T}\to\mathrm{R}}\int_{-\pi}^{\pi} d\gamma\, F_{\mathrm{T}\to\mathrm{R}}(\alpha-\gamma) P_t^T(x-v_{\mathrm{R}}\Delta t\cos\alpha, y-v_{\mathrm{R}}\Delta t\sin\alpha|\gamma),$$

$$P_{t+\Delta t}^T(x,y|\alpha) =$$

$$(1-f_{\mathrm{T}\to\mathrm{R}})\int_{-\pi}^{\pi} d\gamma\, F_{\mathrm{T}}(\alpha-\gamma) P_t^T(x-v_{\mathrm{T}}\Delta t\cos\alpha, y-v_{\mathrm{T}}\Delta t\sin\alpha|\gamma)$$

$$+f_{\mathrm{R}\to\mathrm{T}}\int_{-\pi}^{\pi} d\gamma\, F_{\mathrm{R}\to\mathrm{T}} P_t^R(x-v_{\mathrm{T}}\Delta t\cos\alpha, y-v_{\mathrm{T}}\Delta t\sin\alpha|\gamma).$$

$$(1)$$

Each of the two terms on the right-hand side of the equations represents the possibility of being in one of the two states in the previous time step (see Fig. 1(B) for the particle trajectory during two successive steps). The probability of starting the motion in the run or tumble phase is denoted by P_0^R and P_0^T, respectively (with $P_0^T = 1 - P_0^R$). The change in the direction of motion $\theta = \alpha - \gamma$ with respect to the arrival direction is randomly chosen according to the turning-angle distribution $F_{\mathrm{R}}(\theta)$ or $F_{\mathrm{T}}(\theta)$ in the run or tumble state, respectively. Both distributions are symmetric with respect to the arrival direction (i.e. left-right symmetric in 2D). We assume for simplicity that the directional change during the transition between the two states follows the turning-angle distribution of the new state, corresponding to $F_{\mathrm{R}\to\mathrm{T}}(\theta) = F_{\mathrm{T}}(\theta)$ and $F_{\mathrm{T}\to\mathrm{R}}(\theta) = F_{\mathrm{R}}(\theta)$. However, in general one should consider independent turning-angle distributions with non-zero mean for $F_{\mathrm{R}\to\mathrm{T}}(\theta)$ and $F_{\mathrm{T}\to\mathrm{R}}(\theta)$ as, for instance, a sharp change in the direction of motion of *E. coli* or *Bacillus Subtilis* when switching from tumbling to running is observed [1, 2, 6].

The total probability density $P_{t+\Delta t}(x,y|\alpha)$ to find the particle at position (x,y) arriving along the direction α

at time $t+\Delta t$ is given by $P_{t+\Delta t}(x,y|\alpha) = P^R_{t+\Delta t}(x,y|\alpha) + P^T_{t+\Delta t}(x,y|\alpha)$. Using the Fourier transform of the probability density in each state h ($h \in \{R,T\}$), defined as

$$P^h_{t+\Delta t}(\boldsymbol{k}|m) \equiv \int_{-\pi}^{\pi} d\alpha\, e^{im\alpha} \int dy \int dx\, e^{i\boldsymbol{k}\cdot\boldsymbol{r}} P^h_{t+\Delta t}(x,y|\alpha), \tag{2}$$

the Fourier transform of the total probability density is given by $P_{t+\Delta t}(\boldsymbol{k}|m) = P^R_{t+\Delta t}(\boldsymbol{k}|m) + P^T_{t+\Delta t}(\boldsymbol{k}|m)$, from which the moments of displacement can be calculated as

$$\langle x^{j_1} y^{j_2}\rangle(t+\Delta t) \equiv \int d\alpha \int dy \int dx\, x^{j_1} y^{j_2} P_{t+\Delta t}(x,y|\alpha)$$
$$= (-i)^{j_1+j_2} \left.\frac{\partial^{j_1+j_2} P_{t+\Delta t}(k_x,k_y|m=0)}{\partial k_x^{j_1} \partial k_y^{j_2}}\right|_{(k_x,k_y)=(0,0)}. \tag{3}$$

By means of a Fourier-z-transform technique, it is possible to solve the master equations (1) to obtain the time evolution of the moments of displacement [36, 38, 39]. Here we briefly explain the procedure to calculate the mean square displacement (MSD) as the main quantity of interest. From Eq. (3), the MSD is given as

$$\langle x^2\rangle(t+\Delta t) = (-i)^2 \left.\frac{\partial^2 P_{t+\Delta t}(k,\phi=0|m=0)}{\partial k^2}\right|_{k=0}, \tag{4}$$

where (k,ϕ) is the polar representation of $\boldsymbol{k}$. Assuming $F_{\mathrm{R}\to\mathrm{T}}(\theta)=F_{\mathrm{T}}(\theta)=\frac{1}{2\pi}$ and $F_{\mathrm{T}\to\mathrm{R}}(\theta)=F_{\mathrm{R}}(\theta)$, their Fourier transforms are $F_{\mathrm{R}\to\mathrm{T}}(m)=F_{\mathrm{T}}(m)=\frac{1}{2\pi}\int_{-\pi}^{\pi} d\theta\, e^{im\theta}$ and $F_{\mathrm{T}\to\mathrm{R}}(\theta)=F_{\mathrm{R}}(m)=\int_{-\pi}^{\pi} d\theta\, e^{im\theta} F_{\mathrm{R}}(\theta)$. Next we apply the Fourier transformation on the master equations (1). For example, the first master equation after Fourier transform reads

$$P^R_{t+\Delta t}(k,\phi|m) =$$
$$(1-f_{\mathrm{R}\to\mathrm{T}})\int d\alpha\, e^{im\alpha} \int d\gamma\, F_{\mathrm{R}}(\alpha-\gamma) \int dy \int dx\, e^{i\boldsymbol{k}\cdot\boldsymbol{r}}$$
$$P^R_t(x-v_{\mathrm{R}}\Delta t \cos\alpha, y-v_{\mathrm{R}}\Delta t \sin\alpha|\gamma) \tag{5}$$
$$+ f_{\mathrm{T}\to\mathrm{R}} \int d\alpha\, e^{im\alpha} \int d\gamma\, F_{\mathrm{T}\to\mathrm{R}}(\alpha-\gamma) \int dy \int dx\, e^{i\boldsymbol{k}\cdot\boldsymbol{r}}$$
$$P^T_t(x-v_{\mathrm{R}}\Delta t \cos\alpha, y-v_{\mathrm{R}}\Delta t \sin\alpha|\gamma).$$

Then by using the qth order Bessel's function

$$J_q(z) = \frac{1}{2\pi i^q} \int_{-\pi}^{\pi} d\alpha\, e^{iz\cos\alpha} e^{-iq\alpha},$$

replacing $e^{ikv_{\mathrm{R}}\Delta t \cos(\alpha-\phi)}$ with $\int_{-\pi}^{\pi} d\beta e^{ikv_{\mathrm{R}}\Delta t \cos\beta} \delta(\beta-(\alpha-\phi))$, and using

$$\delta(\beta-(\alpha-\phi)) = \frac{1}{2\pi} \sum_{q=-\infty}^{\infty} e^{-iq(\beta-(\alpha-\phi))},$$

it follows that

$$P^R_{t+\Delta t}(k,\phi|m) = \sum_{q=-\infty}^{\infty} i^q\, e^{-iq\phi} J_q(k\,v_{\mathrm{R}}\Delta t) \times$$
$$\left[(1-f_{\mathrm{R}\to\mathrm{T}})\, F_{\mathrm{R}}(m+q)\, P^R_t(k,\phi|m+q) \right.$$
$$\left. + f_{\mathrm{T}\to\mathrm{R}}\, F_{\mathrm{R}}(m+q)\, P^T_t(k,\phi|m+q)\right]. \tag{6}$$

$P^R_{t+\Delta t}(k,\phi|m)$ can be expanded as a Taylor series

$$P^R_{t+\Delta t}(k,\phi|m) = Q^R_{0,t+\Delta t}(\phi|m) + i\,k\,v_{\mathrm{R}}\,\Delta t\, Q^R_{1,t+\Delta t}(\phi|m)$$
$$- \frac{1}{2}k^2\,v_{\mathrm{R}}^2\,(\Delta t)^2\, Q^R_{2,t+\Delta t}(\phi|m) + \cdots. \tag{7}$$

We expand both sides of Eq. (6) and collect all terms with the same power in k. As a result, recursion relations for the Taylor expansion coefficients can be obtained. For instance, for the terms with power 0 in k one finds

$$Q^R_{0,t+\Delta t}(\phi|m) = (1-f_{\mathrm{R}\to\mathrm{T}})F_{\mathrm{R}}(m)Q^R_{0,t}(\phi|m)$$
$$+ f_{\mathrm{T}\to\mathrm{R}}\, F_{\mathrm{R}}(m)\, Q^T_{0,t}(\phi|m). \tag{8}$$

Similarly, the expansion coefficients of terms with higher powers in k can be calculated and the procedure is repeated for the second master equation in (1). As a result, a set of coupled equations is obtained for each expansion coefficient, connecting time steps $t+\Delta t$ and t. Applying a z-transform $Q(z)=\sum_{t=0}^{\infty} Q_t z^{-t}$ enables one to solve these sets of equations. Particularly the coefficients of terms with power 2 in k, i.e. $Q^R_2(z,\phi|m)$ and $Q^T_2(z,\phi|m)$, are useful to calculate the MSD

$$\langle x^2\rangle(z) = (\Delta t)^2 \left(v_{\mathrm{R}}^2\, Q^R_2(z,0|0) + v_{\mathrm{T}}^2\, Q^T_2(z,0|0)\right). \tag{9}$$

Finally we obtain the following exact expression for the MSD in z space

$$\langle x^2\rangle(z)=\left[\frac{z(1-f_{R\to T}-f_{T\to R})P_0^R}{z-1+f_{R\to T}+f_{T\to R}}+\frac{z^2 f_{T\to R}}{G_0(z)}\right]\left[\frac{z^2}{(z-1)G_1(z)}-\frac{1}{2(z-1)}\right]v_R^2\,(\Delta t)^2+$$
$$\left[\frac{-z(1-f_{R\to T}-f_{T\to R})P_0^R}{z-1+f_{R\to T}+f_{T\to R}}+\frac{z^2(1-f_{T\to R})}{G_0(z)}-\frac{z(1-f_{T\to R}-f_{R\to T})}{G_0(z)}\right]\times$$
$$\left[\frac{z\left[z-(1-f_{R\to T})p\right]}{(z-1)G_1(z)}v_T^2+\frac{z}{(z-1)G_1(z)}f_{T\to R}\,p\,v_R v_T-\frac{1}{2(z-1)}v_T^2\right](\Delta t)^2,\tag{10}$$

where $\quad G_0(z)=(z-1)(z-1+f_{T\to R}+f_{R\to T})\quad$ and $G_1(z)=z\big(z-(1-f_{R\to T})\,p\big)$. By inverse z-transforming Eq. (10), the MSD can be obtained as a function of time. The resulting general expression for the MSD $\langle r^2\rangle(t)=2\langle x^2\rangle(t)$ is lengthy and depends on the run persistency p, the speeds v_R and v_T, the transition probabilities $f_{R\to T}$ and $f_{T\to R}$, and the probability of initially

starting in the run P_0^R or tumble state $P_0^T=1-P_0^R$. $\langle r^2\rangle(t)$ typically consists of linear and exponentially decaying terms with t as well as time-independent terms, as shown in the following in the special case of constant velocity and the initial condition of starting in the run state. By choosing $\Delta t=1$, $v_R=v_T=1$, and the initial condition $P_0^R=1$, the general expression of $\langle r^2\rangle(t)$ reduces to

$$\langle r^2\rangle(t)=\frac{\left(p((f_{T\to R}-1)f_{R\to T}+f_{T\to R}+f_{R\to T}^2)+f_{T\to R}+f_{R\to T}\right)}{p\,(f_{R\to T}-1)(f_{T\to R}+f_{R\to T})+f_{T\to R}+f_{R\to T}}\,t-$$
$$\frac{2\,p\,(f_{R\to T}-1)\big(f_{R\to T}\,p(f_{T\to R}+f_{R\to T}-2)+f_{T\to R}+f_{R\to T}+p-1\big)\big(p(1-f_{R\to T})\big)^t}{\big(p(f_{R\to T}-1)+1\big)^2(f_{T\to R}-f_{R\to T}\,p+f_{R\to T}+p-1)}+$$
$$\frac{2\,p\,f_{R\to T}(1-f_{T\to R}-f_{R\to T})^{t+2}}{(f_{T\to R}+f_{R\to T})^2(f_{T\to R}-f_{R\to T}\,p+f_{R\to T}+p-1)}+$$
$$\frac{\left(p((f_{T\to R}-1)f_{R\to T}+f_{T\to R}+f_{R\to T}^2)+f_{T\to R}+f_{R\to T}\right)}{p\,(f_{R\to T}-1)(f_{T\to R}+f_{R\to T})+f_{T\to R}+f_{R\to T}}-$$
$$\frac{2\,p\big((f_{T\to R}+f_{R\to T})^2-f_{R\to T}\big)+(f_{T\to R}+f_{R\to T})^2}{\big(p\,(f_{R\to T}-1)(f_{T\to R}+f_{R\to T})+f_{T\to R}+f_{R\to T}\big)^2}+$$
$$\frac{p^2(f_{R\to T}-1)\Big((f_{T\to R}+f_{R\to T})\big(f_{T\to R}(f_{R\to T}-1)+(f_{R\to T}-3)f_{R\to T}\big)+2f_{R\to T}\Big)}{\big(p\,(f_{R\to T}-1)(f_{T\to R}+f_{R\to T})+f_{T\to R}+f_{R\to T}\big)^2}.\tag{11}$$

III. RESULTS AND DISCUSSION

We first investigate the time evolution of the MSD for different values of the key parameters p, v_R, v_T, $f_{R\to T}$, $f_{T\to R}$, and P_0^R. As a simple check, the expression (10) for $f_{R\to T}=0$, $f_{T\to R}=1$, $v_T=0$ and $P_0^R=1$ reduces to

$$\langle x^2\rangle(z)=\frac{v_R^2\,z\,(z+p)}{2(z-1)^2\,(z-p)}(\Delta t)^2,\tag{12}$$

and by inverse z-transforming, the MSD for a single-state persistent random walk [35, 40]

$$\langle x^2\rangle(t)=\frac{1}{2}(\Delta t)^2 v_R^2\left[\frac{1+p}{1-p}\,t+2p\frac{p^t-1}{(1-p)^2}\right]\tag{13}$$

is recovered. In Fig. 2, we show how the MSD evolves in time for different values of the key parameters. We plot the general expression of $\langle x^2\rangle(t)$, obtained from the inverse z-transforming of Eq. (10), and validate the analytical predictions by Monte Carlo simulations. A wide range of different types of anomalous dynamics can be observed on varying the parameters. While the short-time dynamics is typically superdiffusion (due to the combination of active and passive motion) and the long-term dynamics is diffusion in all cases, transitions between sub-, ordinary and super-diffusion occur on short and intermediate time scales. For some parameter values, the exponential terms of the MSD rapidly decay while the linear term is not yet big enough compared to the time-independent terms. In such a case, the constant terms dominate at intermediate
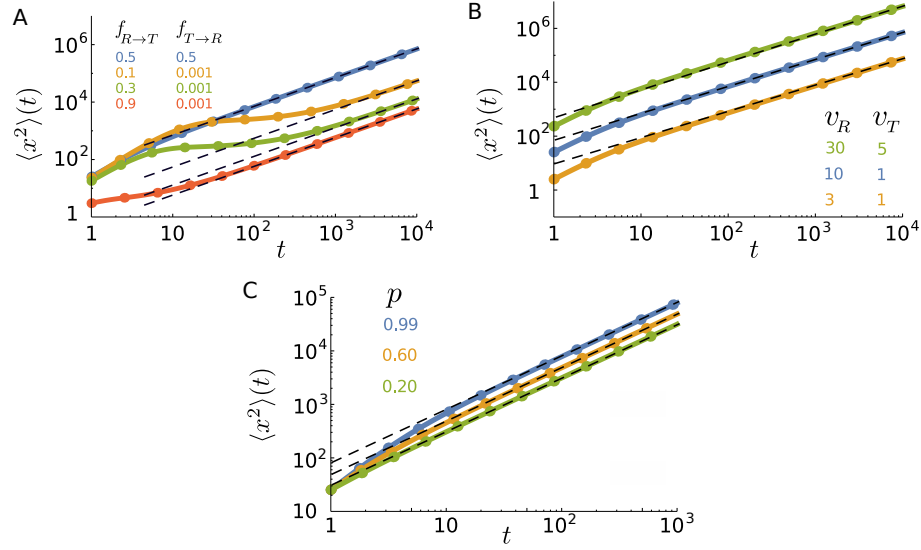
FIG. 2. Time evolution of the MSD for various (A) transition probabilities, (B) speeds, and (C) persistencies. The parameter values (unless varied) are taken to be $p=0.9$, $v_{\mathrm{R}}=10$, $v_{\mathrm{T}}=1$, $\Delta t=1$, $f_{\mathrm{R}\to\mathrm{T}}=0.5$, $f_{\mathrm{T}\to\mathrm{R}}=0.5$ and $P_0^R=0.5$. The lines are obtained from the inverse z-transform of Eq. (10) and symbols denote simulation results. The dashed lines represent the asymptotic diffusion regime.
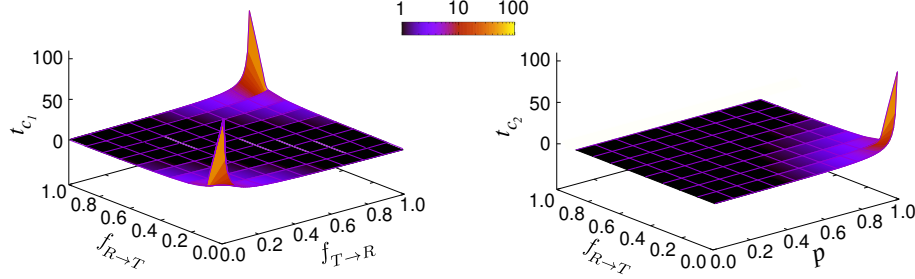

FIG. 3. Characteristic times t_{c_1} and t_{c_2} in terms of the transition probabilities $f_{\mathrm{R}\to\mathrm{T}}$ and $f_{\mathrm{T}\to\mathrm{R}}$ and run persistency p.

time scales leading to the observed slow dynamics in this regime. The asymptotic dynamics is however diffusive since the linear term eventually dominates. It can also be seen that the crossover time to asymptotic diffusion varies by several orders of magnitude upon changing the parameter values. The crossover time can be characterized as the time at which the exponentially decreasing terms in $\langle x^2 \rangle(t)$ become smaller than the terms which survive at long times. We find that the convergence of the MSD to its asymptotic diffusive form can be described by the sum of two exponential functions

$$\langle x^2 \rangle(t) - \langle x^2 \rangle(t\to\infty) \sim B_1\, e^{-t/t_{c_1}} + B_2\, e^{-t/t_{c_2}}, \quad (14)$$

with the characteristic times $t_{c_1}=\dfrac{-1}{\ln\left|1-f_{\mathrm{R}\to\mathrm{T}}-f_{\mathrm{T}\to\mathrm{R}}\right|}$ and $t_{c_2}=\dfrac{-1}{\ln\left|p(1-f_{\mathrm{R}\to\mathrm{T}})\right|}$. The prefactors B_1 and B_2 are functions of p, v_{R}, v_{T}, $f_{\mathrm{R}\to\mathrm{T}}$, $f_{\mathrm{T}\to\mathrm{R}}$, and P_0^R. Figure 3 shows

how the characteristic times t_{c_1} and t_{c_2} vary upon changing the key parameters. Although the slopes of the exponential decays in Eq. (14) are solely determined by the transition probabilities $f_{\mathrm{R}\to\mathrm{T}}$ and $f_{\mathrm{T}\to\mathrm{R}}$ and the run persistency p, the crossover time to the asymptotic diffusive dynamics is also influenced by the other dynamic parameters of the model through the prefactors B_1 and B_2. For example, for the set of parameter values $p=0.9$, $v_{\mathrm{R}}=10$, $v_{\mathrm{T}}=0.1$, $f_{\mathrm{R}\to\mathrm{T}}=0.1$ and $f_{\mathrm{T}\to\mathrm{R}}=0.01$, the convergence time (with 5% accuracy) to the asymptotic dynamics for $P_0^R=1$ is nearly twice as long as for $P_0^R=0$.

Figure 2 also shows that the asymptotic diffusion constant D_{asymp} varies by changing the key parameters. The differences in the y-intercept of the dashed (asymptotic) lines in log-log plots reflect the sensitivity of D_{asymp} to the model parameters. By inverse z-transforming of Eq. (10) and taking the limit $t\to\infty$, we obtain D_{asymp} (i.e. the coefficient of the term linear in time) in the general form as
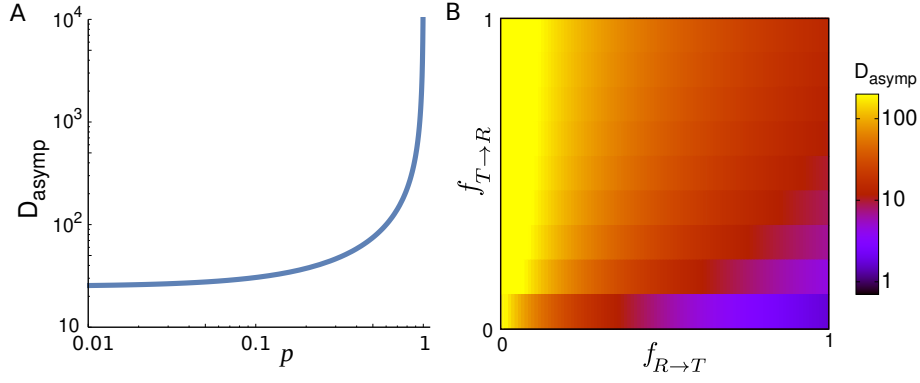
FIG. 4. (A) Asymptotic diffusion coefficient D_asymp as a function of the run persistency p for $v_\mathrm{R}=10$, $v_\mathrm{T}=1$, $\Delta t=1$, $f_{\mathrm{R}\to\mathrm{T}}=0.001$, and $f_{\mathrm{T}\to\mathrm{R}}=0.9$. (B) D_asymp in the space of transition probabilities $f_{\mathrm{R}\to\mathrm{T}}$ and $f_{\mathrm{T}\to\mathrm{R}}$ for $v_\mathrm{R}=10$, $v_\mathrm{T}=1$, $\Delta t=1$, and $p=0.9$.

$$D_\mathrm{asymp} = \frac{1}{4}\,\Delta t\,\frac{2f_{\mathrm{T}\to\mathrm{R}} f_{\mathrm{R}\to\mathrm{T}}\, p\, v_\mathrm{T}\, v_\mathrm{R} + f_{\mathrm{T}\to\mathrm{R}}\, v_\mathrm{R}^2\left(1+p(1-f_{\mathrm{R}\to\mathrm{T}})\right) + f_{\mathrm{R}\to\mathrm{T}}\, v_\mathrm{T}^2\left(1-p(1-f_{\mathrm{R}\to\mathrm{T}})\right)}{\left(f_{\mathrm{T}\to\mathrm{R}}+f_{\mathrm{R}\to\mathrm{T}}\right)\left(1-p(1-f_{\mathrm{R}\to\mathrm{T}})\right)}. \tag{15}$$

While the diffusion coefficient trivially increases with the speed, its dependency on $f_{\mathrm{R}\to\mathrm{T}}$, $f_{\mathrm{T}\to\mathrm{R}}$ and p is more complicated and shown in Fig. 4. D_asymp varies by several orders of magnitude as a function of these parameters. Under the specific condition $F_{\mathrm{R}\to\mathrm{T}}(\theta)=F_\mathrm{T}(\theta)=\delta(\theta)$ and $F_{\mathrm{T}\to\mathrm{R}}(\theta)=F_\mathrm{R}(\theta)$ and $v_\mathrm{T}=0$, the walker stops when entering the tumble phase without changing its arrival direction and it returns smoothly to the run phase without experiencing a kick (i.e. a sharp change in the direction of motion). Motor-driven transport along cytoskeletal filaments in crowded cytoplasm exhibits such a run-and-pause dynamics [21, 41]. In this case, one obtains

$$D_\mathrm{asymp}^\mathrm{run\text{-}pause} = \frac{1}{4}\,\Delta t\, v_\mathrm{R}^2\frac{1+p}{1-p}\frac{f_{\mathrm{T}\to\mathrm{R}}}{f_{\mathrm{T}\to\mathrm{R}}+f_{\mathrm{R}\to\mathrm{T}}}. \tag{16}$$

In the limit $p\to1$ the trajectory becomes nearly straight implying that the randomization time and the covered area until reaching the asymptotic diffusive regime (and thus D_asymp) diverge.

Interestingly, D_asymp in Eq. (15) is independent of P_0^R and P_0^T, i.e. the initial condition of starting the motion in the run or tumble state. Thus the analytical results predict that the asymptotic diffusive dynamics, characterized by the linear time-dependence

$$\langle x^2\rangle(t\to\infty) = 2D_\mathrm{asymp}\, t, \tag{17}$$

does not depend on the initial conditions. In Fig. 5 we

present the simulation results for several values of P_0^R. At long times, all curves merge and follow the analytical prediction Eq. (17). Note that only the linear term in time is independent of P_0^R and the exponentially decaying and time-independent terms in the MSD depend on the initial conditions [see e.g. Eq. (11)]. Although the process is Markovian it keeps initially for some time its memory of the initial direction and state of motion. However, the influence of the P_0^R-dependent terms vanishes in the limit $t\to\infty$ and the time dependence of the MSD appoaches the asymptotic linear form Eq. (17).

The short time dynamics is, however, strongly influenced by the choice of the initial conditions of motion. Figure 5 shows that the initial slope of the MSD curve varies with P_0^R. One can assign an initial anomalous exponent κ to the MSD curve by fitting the power-law $\langle r^2\rangle\sim t^\kappa$. By choosing the first two data points of the MSD curve, the fitting leads to $\langle r^2\rangle(t=2)/\langle r^2\rangle(t=1)=2^\kappa$. Thus, the initial anomalous exponent κ can be deduced from the MSD at $t=1,2$ as

$$\kappa = \ln\left[\frac{\langle r^2\rangle(t=2)}{\langle r^2\rangle(t=1)}\right]/\ln2, \tag{18}$$

After replacing the MSD at $t=1,2$ obtained from Eq. (10) we get

$$\kappa = \ln\left[\left[\left(2-2P_0^R+(3-f_{\text{T}\rightarrow\text{R}}-f_{\text{R}\rightarrow\text{T}})(f_{\text{T}\rightarrow\text{R}}(P_0^R-1)+f_{\text{R}\rightarrow\text{T}}P_0^R)\right)v_{\text{T}}^2+\right.\right.$$

$$2f_{\text{T}\rightarrow\text{R}}\left(1-f_{\text{T}\rightarrow\text{R}}+(f_{\text{T}\rightarrow\text{R}}+f_{\text{R}\rightarrow\text{T}}-1)P_0^R\right)p\,v_{\text{T}}\,v_{\text{R}}+$$

$$\left(2P_0^R+(-3+f_{\text{T}\rightarrow\text{R}}+f_{\text{R}\rightarrow\text{T}})(f_{\text{T}\rightarrow\text{R}}(P_0^R-1)+f_{\text{R}\rightarrow\text{T}}P_0^R)+\right.$$

$$\left.\left.2(f_{\text{R}\rightarrow\text{T}}-1)\left(-f_{\text{T}\rightarrow\text{R}}+(f_{\text{T}\rightarrow\text{R}}+f_{\text{R}\rightarrow\text{T}}-1)P_0^R\right)p\right)v_{\text{R}}^2\right]/ \tag{19}$$

$$\left.\left[\left(1-f_{\text{T}\rightarrow\text{R}}-(1-f_{\text{T}\rightarrow\text{R}}-f_{\text{R}\rightarrow\text{T}})P_0^R\right)v_{\text{T}}^2+\left(f_{\text{T}\rightarrow\text{R}}+(1-f_{\text{T}\rightarrow\text{R}}-f_{\text{R}\rightarrow\text{T}})P_0^R\right)v_{\text{R}}^2\right]\right]/\ln 2.$$
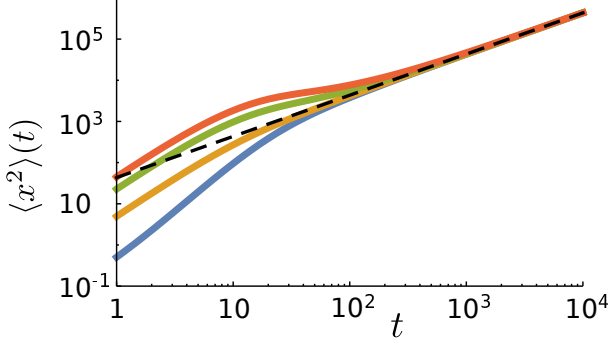

FIG. 5. The mean square displacement as a function of time for different values of the probability P_0^R of initially starting in the run state in simulations (from top to bottom: $P_0^R=1.0, 0.5, 0.1, 0.0$). Other parameter values: $p=0.9$, $v_{\text{R}}=10$, $v_{\text{T}}=0.1$, $f_{\text{R}\rightarrow\text{T}}=0.1$ and $f_{\text{T}\rightarrow\text{R}}=0.01$. The dashed line represents the analytical prediction via Eq. (17) for the same parameter values.

ing other parameter values. However, κ increases monotonically with p in all parameter regimes as shown in Fig. 6(B). Moreover, figures 6(C) and (D) show that κ also varies widely with the speed and transition probabilities. Because of combining an active run state ($0<p<1$) and normal diffusion (tumble state), κ remains above 1 (superdiffusion). However, by generalizing the run state to include subdiffusive motion (i.e. when $-1<p<1$), κ can decrease below 1.

To better understand the role of the initial conditions, we note that the steady probabilities P_{steady}^R and P_{steady}^T of finding the particle in each of the two states is determined by the transition probabilities $f_{\text{R}\rightarrow\text{T}}$ and $f_{\text{T}\rightarrow\text{R}}$. Therefore, the influence of the initial condition of starting the motion in any of the two states gradually vanishes as the probabilities $P^R(t)$ and $P^T(t)$ of finding the particle in the run or tumble state gradually approach their steady values. By considering a discrete time Markov process with transition probabilities $f_{\text{R}\rightarrow\text{T}}$ and $f_{\text{T}\rightarrow\text{R}}$, the probabilities at time t can be obtained from those at time $t-1$ as

$$\left(P^R(t), P^T(t)\right) = \left(P^R(t-1), P^T(t-1)\right)\begin{bmatrix}1-f_{\text{R}\rightarrow\text{T}} & f_{\text{R}\rightarrow\text{T}} \\ f_{\text{T}\rightarrow\text{R}} & 1-f_{\text{T}\rightarrow\text{R}}\end{bmatrix}. \tag{20}$$

By applying this relation recursively, one can derive the probabilities at time t based on the initial probabilities

Figure 6(A) shows how the initial conditions of motion influences the initial anomalous exponent for a given set of parameters. Note that the displayed monotonic growth of κ with P_0^R does not hold in general, as we observed decreasing as well as nonmonotonic functionalities by varying.

$$\left(P^R(t), P^T(t)\right) = \left(P_0^R, P_0^T\right)\begin{bmatrix}1-f_{\text{R}\rightarrow\text{T}} & f_{\text{R}\rightarrow\text{T}} \\ f_{\text{T}\rightarrow\text{R}} & 1-f_{\text{T}\rightarrow\text{R}}\end{bmatrix}^t$$

$$= \left(P_0^R, P_0^T\right)\frac{1}{f_{\text{R}\rightarrow\text{T}}+f_{\text{T}\rightarrow\text{R}}}\begin{bmatrix}f_{\text{T}\rightarrow\text{R}}+f_{\text{R}\rightarrow\text{T}}(1-f_{\text{T}\rightarrow\text{R}}-f_{\text{R}\rightarrow\text{T}})^t & f_{\text{R}\rightarrow\text{T}}\left(1-(1-f_{\text{T}\rightarrow\text{R}}-f_{\text{R}\rightarrow\text{T}})^t\right) \\ f_{\text{T}\rightarrow\text{R}}\left(1-(1-f_{\text{T}\rightarrow\text{R}}-f_{\text{R}\rightarrow\text{T}})^t\right) & f_{\text{R}\rightarrow\text{T}}+f_{\text{T}\rightarrow\text{R}}(1-f_{\text{T}\rightarrow\text{R}}-f_{\text{R}\rightarrow\text{T}})^t\end{bmatrix}. \tag{21}$$

Thus the evolution of $P^R(t)$ and $P^T(t)$ obeys

$$P^R(t) = \frac{f_{\text{T}\rightarrow\text{R}}}{f_{\text{T}\rightarrow\text{R}}+f_{\text{R}\rightarrow\text{T}}} + \frac{\left(1-f_{\text{T}\rightarrow\text{R}}-f_{\text{R}\rightarrow\text{T}}\right)^t}{f_{\text{T}\rightarrow\text{R}}+f_{\text{R}\rightarrow\text{T}}}\left(f_{\text{R}\rightarrow\text{T}}P_0^R-f_{\text{T}\rightarrow\text{R}}(1-P_0^R)\right),$$

$$P^T(t) = \frac{f_{\text{R}\rightarrow\text{T}}}{f_{\text{T}\rightarrow\text{R}}+f_{\text{R}\rightarrow\text{T}}} - \frac{\left(1-f_{\text{T}\rightarrow\text{R}}-f_{\text{R}\rightarrow\text{T}}\right)^t}{f_{\text{T}\rightarrow\text{R}}+f_{\text{R}\rightarrow\text{T}}}\left(f_{\text{R}\rightarrow\text{T}}P_0^R-f_{\text{T}\rightarrow\text{R}}(1-P_0^R)\right), \tag{22}$$
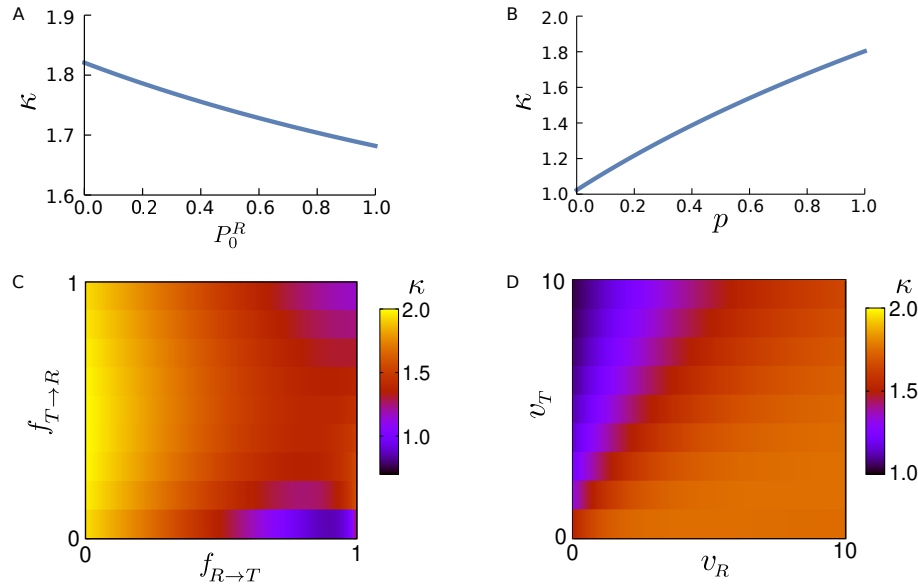
FIG. 6. The anomalous exponent κ versus (A) the initial condition of motion P_0^R, (B) run persistency p, (C) transition probabilities $f_{R\to T}$ and $f_{T\to R}$, and (D) speeds v_R and v_T via Eq. (19). The parameter values (unless varied) are taken to be $p=0.9$, $v_R=10$, $v_T=1$, $\Delta t=1$, $f_{R\to T}=0.3$, $f_{T\to R}=0.5$ and $P_0^R=0.5$.

leading to the steady probabilities $P_{\text{steady}}^R = \frac{f_{T\to R}}{f_{T\to R}+f_{R\to T}}$ and $P_{\text{steady}}^T = \frac{f_{R\to T}}{f_{T\to R}+f_{R\to T}}$. If one starts with the initial condition $P_0^R = P_{\text{steady}}^R$, the system is immediately equilibrated. Otherwise, the choice of the initial conditions of motion affects the short-time dynamics and diversifies the transient anomalous diffusive regimes. According to Eq. (22), the relaxation of the probabilities toward their steady values follow an exponential decay $P^R(t)$, $P^T(t) \sim e^{-t/t_m}$ with $t_m = \frac{-1}{\ln|1-f_{R\to T}-f_{T\to R}|}$. While the characteristic time for the relaxation of the probabilities solely depends on the transition probabilities, the characteristic time for the crossover to asymptotic dynamics is influenced additionally by the run persistency, as we showed previously in Eq. (14). Therefore, there are two independent relaxation times $t_m(=t_{c_1})$ and t_{c_2}. In case the relaxations occur on different time scales, two distinct crossovers in the time evolution of the MSD may be observed in general as can be seen in Fig. 2(A).

IV. CONCLUSION

We presented a persistent random walk model to study the stochastic dynamics of particles with active fast and passive slow motility modes. We derived an exact analytical expression for the mean square displacement, which allows one to analyze the transient anomalous transport regimes on short time scales and also extract the characteristics of the asymptotic diffusive motion such as the crossover time and the long-term diffusion constant. In particular we showed that while the choice of the initial conditions of motion influences the anomalous diffusion at short times, the asymptotic behavior remains independent of it and is entirely controlled by the run persistency, the velocities of the run and tumble states and the transition probabilities between the two states.

[1] H. C. Berg, *E. coli in motion* (Springer Verlag, New York, 2004).

[2] H. C. Berg and D. A. Brown, Nature **239**, 500 (1972), URL https://www.nature.com/articles/239500a0.

[3] A. E. Patteson, A. Gopinath, M. Goulian, and P. E. Arratia, Sci. Rep. **5**, 15761 (2015), URL https://www.nature.com/articles/srep15761.

[4] F. Bartumeus and S. A. Levin, Proc. Natl. Acad. Sci. USA **105**, 19072 (2008), ISSN 0027-8424, https://www.pnas.org/content/105/49/19072.full.pdf, URL https://www.pnas.org/content/105/49/19072.

[5] O. Bénichou, M. Coppey, M. Moreau, P.-H. Suet, and R. Voituriez, Phys. Rev. Lett. **94**, 198101 (2005), URL https://link.aps.org/doi/10.1103/PhysRevLett.94.198101.

[6] J. Najafi, M. R. Shaebani, T. John, F. Altegoer, G. Bange, and C. Wagner, Sci-

ence Adv. **4**, eaar6425 (2018), URL http://advances.sciencemag.org/content/4/9/eaar6425.

[7] O. Bénichou, C. Loverdo, M. Moreau, and R. Voituriez, Rev. Mod. Phys. **83**, 81 (2011), URL https://link.aps.org/doi/10.1103/RevModPhys.83.81.

[8] G. H. Wadhams and J. P. Armitage, Nat. Rev. Mol. Cell Biol. **5**, 1024 (2004), URL https://www.nature.com/articles/nrm1524.

[9] J. Taktikos, H. Stark, and V. Zaburdaev, PLoS ONE **8**, 1 (2014), URL https://doi.org/10.1371/journal.pone.0081936.

[10] A. V. Weigel, B. Simon, M. M. Tamkun, and D. Krapf, Proc. Natl. Acad. Sci. USA **108**, 6438 (2011), ISSN 0027-8424, URL https://www.pnas.org/content/108/16/6438.

[11] G. Guigas and M. Weiss, Biophys. J. **94**, 90 (2008), ISSN 0006-3495, URL http://www.sciencedirect.com/science/article/pii/S0006349508070677.

[12] I. Golding and E. C. Cox, Phys. Rev. Lett. **96**, 098102 (2006), URL https://link.aps.org/doi/10.1103/PhysRevLett.96.098102.

[13] L. E. Sereshki, M. A. Lomholt, and R. Metzler, EPL **97**, 20008 (2012), URL https://doi.org/10.1209%2F0295-5075%2F97%2F20008.

[14] M. Y. Ali, E. B. Krementsova, G. G. Kennedy, R. Mahaffy, T. D. Pollard, K. M. Trybus, and D. M. Warshaw, Proc. Natl. Acad. Sci. USA **104**, 4332 (2007), ISSN 0027-8424, URL https://www.pnas.org/content/104/11/4332.

[15] K. Shiroguchi and K. Kinosita, Science **316**, 1208 (2007), ISSN 0036-8075, URL https://science.sciencemag.org/content/316/5828/1208.

[16] M. Vershinin, B. C. Carter, D. S. Razafsky, S. J. King, and S. P. Gross, Proc. Natl. Acad. Sci. USA **104**, 87 (2007), ISSN 0027-8424, URL https://www.pnas.org/content/104/1/87.

[17] Y. Okada, H. Higuchi, and N. Hirokawa, Nature **424**, 574 (2003), URL https://www.nature.com/articles/nature01804.

[18] T. L. Culver-Hanlon, S. A. Lex, A. D. Stephens, N. J. Quintyne, and S. J. King, Nat. Cell Biol. **8**, 264 (2006), URL https://www.nature.com/articles/ncb1370.

[19] S. Klumpp and R. Lipowsky, Phys. Rev. Lett. **95**, 268102 (2005), URL https://link.aps.org/doi/10.1103/PhysRevLett.95.268102.

[20] R. Lipowsky and S. Klumpp, Physica A **352**, 53 (2005), ISSN 0378-4371, URL http://www.sciencedirect.com/science/article/pii/S0378437104016176.

[21] A. E. Hafner, L. Santen, H. Rieger, and M. R. Shaebani, Sci. Rep. **6**, 37162 (2016), URL https://www.nature.com/articles/srep37162.

[22] I. Pinkoviezky and N. S. Gov, Phys. Rev. E **88**, 022714 (2013), URL https://link.aps.org/doi/10.1103/PhysRevE.88.022714.

[23] M. Chabaud and et al., Nat. Commun. **6**, 7526 (2015), URL https://www.nature.com/articles/ncomms8526.

[24] P. C. Bressloff and J. M. Newby, Rev. Mod. Phys. **85**, 135 (2013), URL https://link.aps.org/doi/10.1103/RevModPhys.85.135.

[25] F. Höfling and T. Franosch, Rep. Prog. Phys. **76**, 046602 (2013), URL https://doi.org/10.1088%2F0034-4885%2F76%2F4%2F046602.

[26] L. Angelani, EPL **102**, 20004 (2013), URL https://doi.org/10.1209%2F0295-5075%2F102%2F20004.

[27] R. Soto and R. Golestanian, Phys. Rev. E **89**, 012706 (2014), URL https://link.aps.org/doi/10.1103/PhysRevE.89.012706.

[28] M. R. Shaebani, A. Pasula, A. Ott, and L. Santen, Sci. Rep. **6**, 30285 (2016), URL https://www.nature.com/articles/srep30285.

[29] M. Theves, J. Taktikos, V. Zaburdaev, and C. Beta, Biophys. J. **105**, 1915 (2013), ISSN 0006-3495, URL http://www.sciencedirect.com/science/article/pii/S0006349513010916.

[30] J. Elgeti and G. Gompper, EPL **109**, 58003 (2015), URL https://doi.org/10.1209%2F0295-5075%2F109%2F58003.

[31] F. Thiel, L. Schimansky-Geier, and I. M. Sokolov, Phys. Rev. E **86**, 021117 (2012), URL https://link.aps.org/doi/10.1103/PhysRevE.86.021117.

[32] O. G. Berg, R. B. Winter, and P. H. Von Hippel, Biochem **20**, 6929 (1981), ISSN 0006-2960, URL https://doi.org/10.1021/bi00527a028.

[33] Y. Meroz, I. Eliazar, and J. Klafter, J. Phys. A **42**, 434012 (2009), URL https://doi.org/10.1088%2F1751-8113%2F42%2F43%2F434012.

[34] M. Bauer and R. Metzler, Biophy. J. **102**, 2321 (2012), ISSN 0006-3495, URL http://www.sciencedirect.com/science/article/pii/S0006349512004237.

[35] R. Nossal and G. H. Weiss, J. Theor. Biol. **47**, 103 (1974), ISSN 0022-5193, URL http://www.sciencedirect.com/science/article/pii/0022519374901010.

[36] Z. Sadjadi, M. R. Shaebani, H. Rieger, and L. Santen, Phys. Rev. E **91**, 062715 (2015), URL https://link.aps.org/doi/10.1103/PhysRevE.91.062715.

[37] M. R. Shaebani and Z. Sadjadi, submitted (2019).

[38] Z. Sadjadi, M. Miri, M. R. Shaebani, and S. Nakhaee, Phys. Rev. E **78**, 031121 (2008), URL https://link.aps.org/doi/10.1103/PhysRevE.78.031121.

[39] M. R. Shaebani, Z. Sadjadi, I. M. Sokolov, H. Rieger, and L. Santen, Phys. Rev. E **90**, 030701 (2014), URL https://link.aps.org/doi/10.1103/PhysRevE.90.030701.

[40] and M. R. Shaebani, Soft Matter **12**, 3398 (2016), URL http://dx.doi.org/10.1039/C6SM00237D.

[41] M. S. Song, H. C. Moon, J.-H. Jeon, and H. Y. Park, Nat. Commun. **9**, 344 (2018), ISSN 2041-1723, URL https://doi.org/10.1038/s41467-017-02700-z.